Analysis by computed microtomography of pore characteristics effects on the permeability of *Dalbergia ruddae* wood

J.G. Rivera-Ramos[1], R. Espinoza-Herrera[1], J. Cruz de León[1], D. Arteaga[2]

[1] Universidad Michoacana de San Nicolás de Hidalgo, Fco. J. Mujica S/N, Morelia, C.P. 58060, México
[2] Universidad Nacional Autónoma de México, Blvd. Juriquilla No. 3001. Querétaro, 76230, México.

Aims

Infiltration of woods with different substance is widely used for both improving mechanical properties or increasing its resistance to fungal or insects attack. Interaction between the properties of the fluid and the characteristics of the wood microstructure largely determine the flow behavior during infiltration. The biometric characteristics of the wood porosity is one of the most influential factors. Porosity can present obstructions due to natural processes or drying treatments, preventing the penetration and adequate distribution of infiltration fluids. In addition, the retention of such fluids and that related to the type of porosity is not entirely clear because more of the works about it have been developed by 2D post mortem analysis, as a consequence of that the existing models do not adequately describe this interaction. Hence, it is important to know the biometric characteristics of wood and its interaction with fluids. Recently, numerical simulations have been used to understand the behavior of the fluid in a porous structure. Therefore, the objective of the present investigation is to characterize the porosity features involved in the internal fluid flow of wood by coupling three-dimensional micro-CT image analysis with numerical computational simulations.

Method

3D images were acquired from a wood specimen of *Dalbergia ruddae* with a diameter of 1 mm, which is determined according to the size of the plant tissue cells, thus the resulting voxel size was 1.09 µm. The acquisition was carried out on a Xradia Zeiss Versa 510 tomography equipment that uses a camera of 1024 x 1024 pixels as detector. The X-ray voltage used was of 50 Kv and 1600 radiographs were taken at an angular displacement of 0.225° around the sample, with an exposure time of 6s. The image obtained has the following dimensions 993 x 988 x 1015 pixels.

Image analysis and numerical permeability simulations were performed with the aid of commercial softwares like ImageJ and AVIZO®, respectively. Subvolumes from the center of the initial 3D image were virtually extracted for analysis in order to reduce the computing time. The procedure for the measurements of the cellular cell, wall thickness and volume fraction of wood is the one described in [1]. The methodology for the measurement of pore area, geometric tortuosity and permeability in the direction parallel to the orientation of the tree axis is described in [2]. The permeability simulations were performed at a fluid viscosity of 0.001 Pa s, and constant pressure differential of 30000 Pa with Avizo. Besides, the simulations were also carried out in the different voids of the wood separately, on vessel cells, and parenchyma cells and wood fibers. This allows to know additional information of the complexity for the fluid to pass throughout each one.

Results

Segmented images allow to measure the different kind of cellular tissues that compose the wood (Figure 1a). In addition, the both kind of pores (vessel and pores) are individually shown in Figure 2b, as well as the solid phase that represents the fibers of wood (Figure 1b). Likewise, because the images reflect the heterogeneity of the anatomical structure of the wood, porosity and cell wall thickness distributions were acquired. Pore concentrations with surfaces less than 50 μm^2 are observed (Figure 2a). With 7.6, 4.9, 5.1, 3.1 and 3.3 % for surfaces of 10.6, 14.2, 17.8, 22.5 and 26.1 μm^2, respectively. These surfaces correspond mainly to the lumen cells, meanwhile the larger values of surface correspond to the pore vessel surfaces (18868.2 μm^2). The magnitude of concentration of small surfaces can largely determine the level of complexity of a cellular tissue to the passage of a fluid [3].

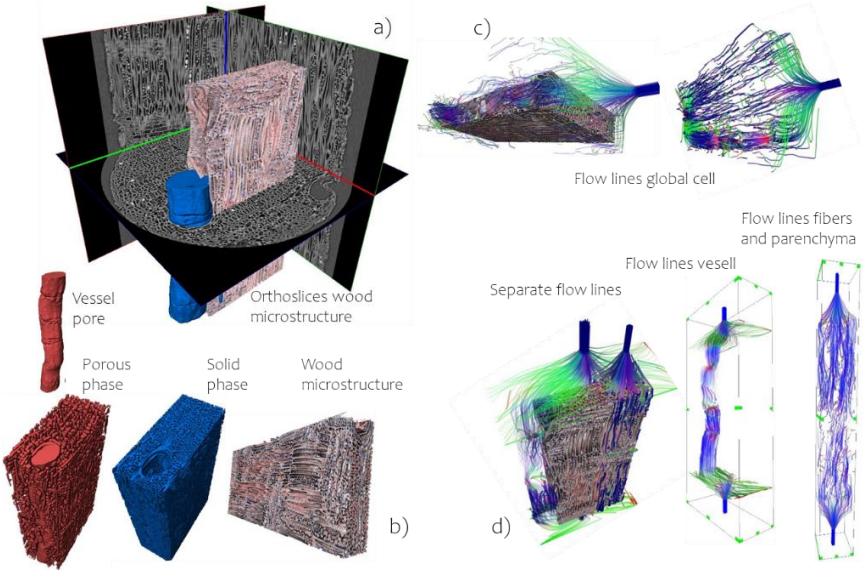

Figure 1: a) 2D multi ortho slices and 3D rendenring of the vessels and wood's microstructure. b) 3D rendering of the different elements that compose the wood's microstructure. c) and d) Simulated flow lines throughout the porosity of the *Dalbergia* ruddae wood.

The solid phase that corresponds to the cellular wall of wood was also measured from 3D images. The wall thicknesses are distributed from 1.2 to 14 µm (Figure 2b). It was pointed out that small thicknesses can develop defects and potentially obstruct the pass of fluids during the drying of woods [4].

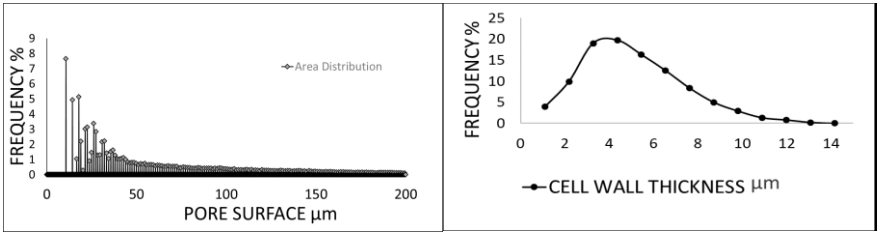

Figure 2: a) pore surface distribution and b) cell wall thicknesses distribution.

The global value of permeability axial calculated from numerical simulations is 17.9 μm^2, as listed in Table 1. This value is similar to the one calculated for the parenchyma and fiber cells, 17.9 μm^2, which is three times larger than the one calculated for the vessel cells, 6.1 μm^2. This indicates that most of fluid pass throughout the parenchyma and fiber cells instead of vessels (Figure 1c), which is contrary to the expected result. However, it is explained because it is observed the presence of a tissue obstructing the flow in the vessel capillaries, which is detected by a red colour on the flow lines along the vessel, which indicates that velocity of flow is increased at that zone by forcing the fluid to pass throughout the small pores of the cellular pitts that are smaller diamters that the rest of the wood tissue (Figure 1c). The results also show that the participation of fiber capillaries and parenchyma is determinant for the fluid flow when the vessels are obstructed (Figure 1d). The geometric tortuosity for the vessel and the rest of the tissue is barely the same, which wasn't expected. Thus, the permeability is not affected by this parameter (Table 1). The pore volume fraction of the analyzed volume is much higher than the solid phase obtained (Table 1), this characteristic is typical of this species due to the large number of parenchyma cell capillaries (Figure 1a). The pore volume fraction of the parenchyma and fiber cells is 8 times to the one of the vessel cells, which plays a major role on the permeability since the quantity of pores has widely linked to an increment on the permeability. According to the numerical simulations performed, the participation in the flow of this extensive parenchyma capillary system is important for this timber species.

Table 1. Porosity characteristics of the *Dalbergia Ruddae* Wood

	Parenchyma-Fiber cells	**Vessel cells**	**Global cell of wood**	**Cellular wall**
Axial Permeability (μm^2)	17.998	6.139	17.973	-
Geometric Tortuosity	1.180	1.056	1.174	-
Volumen fraction (%)	55.199	7.386	62.586	37.42

Conclusion

The pore characteristics of wood show a reduction effect on axial permeability caused by the reduction of surfaces sections in the vessels and the clogging of vessels leading to deviations in the trajectories of the flow throughout the cellular tissue of the wood. Computed tomography allowed a realistic analysis of the complexity of void spaces, porosity, in wood to determine the passage of fluids through it.

References:

1. Olmos, N.L.R.; Espinoza, H.R.; Cruz-de-León, J. & Hernández, V.A., ”Caracterización microestructural 3D de la madera de Pithecellobium pallens mediante microtomografía de rayos X”. Memorias del XXII Congreso de la SOMIM. Mérida, Yucatán, México, 2016
2. Rivera Ramos, J. G., Espinoza Herrera, R., Arteaga, D., Cruz de León, J., & Olmos, L.,”Microstructural analysis of Eucalyptusnitens wood through computed microtomography”. Wood Material Science & Engineering, 1-14, 2020
3. Zimmer, K., Treu, A., & McCulloh, K. A.,” Anatomical differences in the structural elements of fluid passage of Scots pine sapwood with contrasting treatability”. Wood science and technology, 48(2), 435-447, 2014
4. Usta I. “A review of the configuration of bordered pits to stimulate the fluid flow”. Maderas-Ciencia Tecnologia, 7(2):121–132, 2005